# Magnesium Hydride: From the Laboratory to the Tank

Jean-Gabriel Roquefere and Jean-Louis Bobet

Institut de Chimie de la Matière Condensée de Bordeaux, ICMCB, CNRS [UPR 9048], Université Bordeaux 1, 87 Avenue du Dr A. Schweitzer. 33608 Pessac cedex, France

Reprint requests to Prof. Jean-Louis Bobet. Fax: +33-(0)5-4000-2761.
E-mail: bobet@icmcb-bordeaux.cnrs.fr

*Z. Naturforsch.* **2007**, *62b,* 907 – 914; received February 19, 2007

*Dedicated to Dr. Bernard Chevalier on the occasion of his 60$^{th}$ birthday*

Magnesium metal is under extensive study for its high hydrogen absorption capacity. The main results obtained by the authors, going from the effects of 'reactive mechanical grinding' to the addition of nano oxides or to the deposition of nanoparticles are reported and discussed. The absorption properties are compared with the results of other research groups. An improvement of kinetics has been achieved and the mechanisms of the hydrogenation reaction is almost fully understood, but the effects of catalysts are still subject to hypotheses. Recent developments of $MgH_2$ tanks are also presented.

*Key words:* Magnesium Hydride, Milling under Hydrogen, Hydrogen Storage, Diffusion and Nucleation Process, Hydrogen Tank

## Introduction

The green house gas emission by burning fossil fuels is becoming a serious problem and the effects on the climate are already visible. For example, the grape harvest dates are now about 30 days ahead of those 50 years ago. Clean sources of energy are becoming more and more important. Hydrogen is often considered as the energy vector of the future. Research has been focused on two main problems associated with the use of hydrogen: (i) mass production of carbon-free hydrogen and (ii) storage of hydrogen. For their high capacities and low hazards of handling, metal hydrides appear to offer the best opportunities. Magnesium in particular has the highest absorption capacity, but its major drawback is that the absorption kinetics are very slow and the dissociation temperature of $MgH_2$ is rather high [1, 2]. The most usual way to improve the absorption/desorption kinetics is the addition of metals or alloys to Mg using high-energy ball milling [3]. A large variety of additives have been used such as metals, intermetallics, non metals and oxides [4 – 14]. In this paper, we review the major work carried out in our laboratory within the last ten years in the fields of (i) improving the absorption properties of magnesium, as well as (ii) understanding the kinetic behaviour.

## Experimental Details

Pure Mg powder was ball-milled with various elements using a P5 miller with a rotation speed of 300 rpm in most cases. The hydrogen pressure in the vial was fixed at 1.1 MPa and was renewed every 30 min to avoid the loss of pressure due to absorption and possible leaks.

The crystalline structure of the as-milled powders was characterized by X-ray diffraction (XRD) analysis on a Philips PW 1050 diffractometer using the Bragg-Brentano geometry (Cu$K_\alpha$ radiation). These patterns were scanned per steps of 0.02° ($2\theta$) from 15 to 80° with a counting time of 10 s. The diffraction patterns were analyzed by a fitting procedure (with the Thomson-Cox-Hastings function) using the program FULLPROF [15] in order to determine the lattice parameters, the relative weight content of each phase and both the crystallite size and the internal strains. The hydriding apparatus has been described previously [11].

SEM was carried out with a JEOL JSM 840 instrument operating at an acceleration voltage of 20 kV. The energy-dispersive X-ray (EDX) analysis was performed with a Noran spectrometer (Voyager 4 system) coupled with the SEM. Size measurements were performed using a Malvern Mastersizer Hydro 2000S in liquid (ethanol) media. The sample (20 mg) was dispersed in ethanol using an ultrasonic device (47 kHz, 125 W, 30 min). Additional characterizations such as EPMA (CAMECA SX-100 Instrument) and Zeta potential (Malvern Z3000) were carried out before and after cycling.

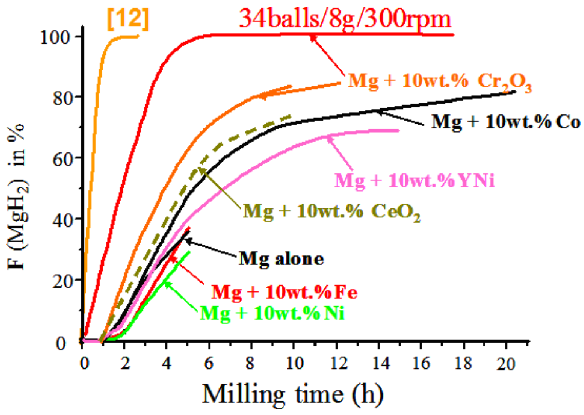


Fig. 1. Estimation (from Rietveld refinement analysis) of the fraction of $MgH_2$ formed during the milling process.

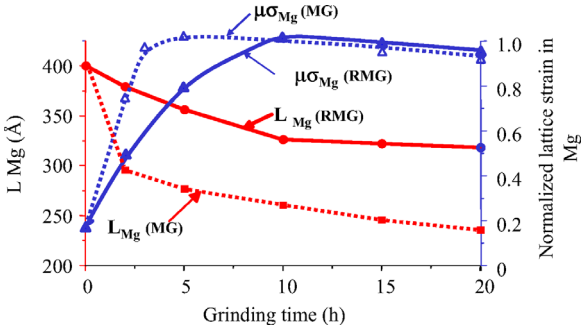


Fig. 2. Evolution of both the lattice strain and the crystallite size during the milling process for the mixtures Mg + 10 % Co ball-milled under both $H_2$ and Ar at 200 rpm.

## Results and Discussion

### *RMG Effects on Mg*

Reactive mechanical grinding (RMG = grinding under reactive gas atmosphere, here hydrogen) has been recognized to be a useful tool for the milling of the very ductile magnesium. Due to the ductility of magnesium, most of the published work on ball milling of magnesium is in fact concerning the ball milling of magnesium hydride. We have developed and optimized a reactive ball milling process by which $MgH_2$ is formed *in situ* during milling. Our first investigation was concerned with the rate of formation of $MgH_2$ during the milling process. The major results are summarized in Fig. 1.

The figure clearly shows that the additives do not much influence the fraction of $MgH_2$ formed. However, it is obvious that the more brittle the additives, the higher the fraction of $MgH_2$ formed. The brittle constituent acts as an abrasive during the milling process, improving the efficiency of the milling. In order to increase the milling efficiency, we changed both the rotation speed and the number of balls in the vials. Then, for the same mixtures (*i. e.* Mg + 10 % $Cr_2O_3$) it was possible to reach a full conversion of Mg into $MgH_2$ in 5 h with a rotation speed of 300 rpm and with 34 balls, whereas at 200 rpm and with 17 balls, the fraction of $MgH_2$ was only about 80 % after 10 h. Liang *et al.* [12] have even reached a full conversion in less than an hour by heating the vials to 200 °C during milling. In this last case the milling energy is added to the thermal energy and thus the hydrogenation of magnesium becomes very fast.

As the efficiency of ball milling was the key parameter, it was of prime importance to find a tool to evaluate this efficiency. Fig. 2 presents the evolution of the lattice strain and the size of the crystallites as determined by XRD analysis.

For samples ball-milled in an $H_2$ atmosphere, it appears that the lattice strains increase gradually up to 10 h of milling and thereafter reach an upper limit. Beyond 10 h, they remain almost constant and just a slight decrease can be noticed. The decrease of the crystallite size corresponds to the increase in the lattice strains. When the lattice strains reach their maximum value, the crystallite size reaches its minimum value and remains almost constant. The fraction of $MgH_2$ formed during milling (see Fig. 1) behaves in the same way as the lattice strains. After 10 h, the fraction of $MgH_2$ formed is 66 %, and it is only 74 % after 20 h. The milling thus is less efficient after 10 h. The process of the $MgH_2$ formation could be assumed to start with adsorption of hydrogen on particles created by crushing (fresh surface) followed by diffusion of the adsorbed hydrogen into the metal to form the metal hydride. The milling efficiency beyond 10 h is low because no fresh surface is created and the rate of formation of $MgH_2$ is considerably reduced. In the case of ball milling under Ar, the efficiency of milling beyond 3 h is low because of the sticking of Mg to the walls of the vials.

### *Hydrogen absorption and desorption properties of various mixtures*

In Fig. 3, the desorption properties of various Mg + *M* mixtures are shown. The effects of the crystallite size of Mg (or $MgH_2$) is clearly highlighted in this figure. The product of ball-milled Mg metal exhibits

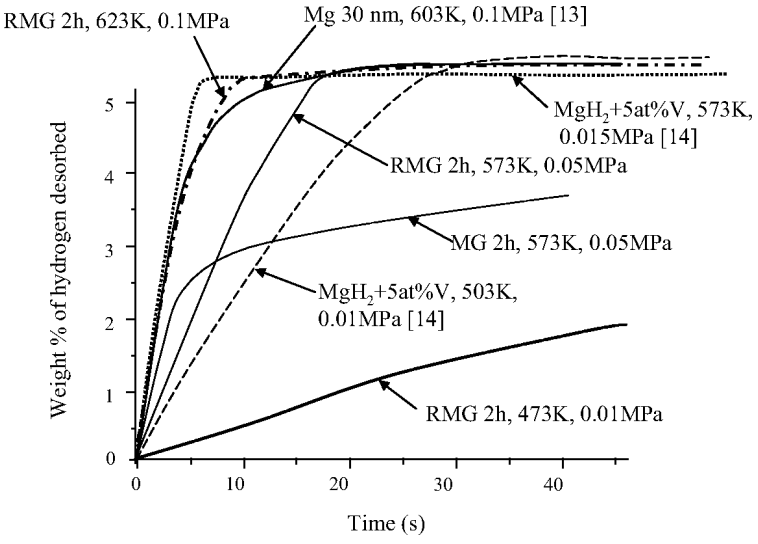


Fig. 3. Hydrogen desorption curves under various pressure and temperature conditions for Mg + 10 wt. % Co subjected to RMG or MG (mechanical grinding) processes. A comparison with the data obtained by Zaluski *et al*. [13] and Liang *et al*. [14] (both dotted lines) is included.

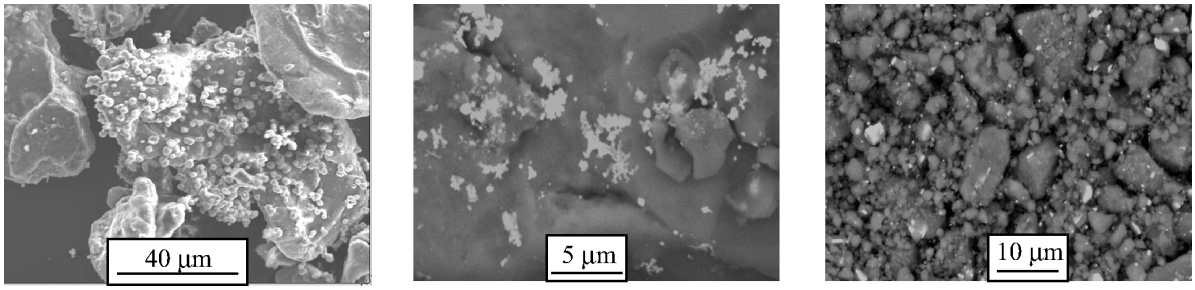


Fig. 4. SEM images of Mg + Ni (SCF) (left), Mg + Pd (SCF) (centre) and Mg + Pd ball-milled for 10 h (right).

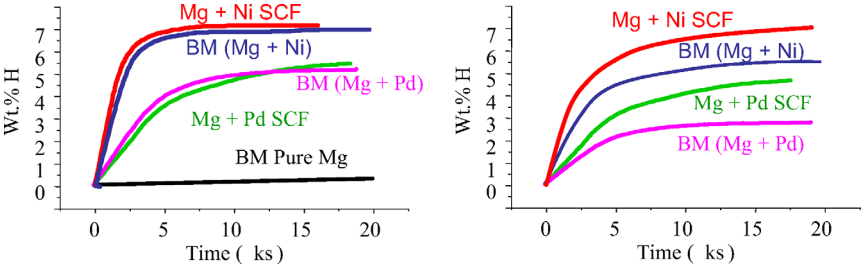


Fig. 5. Hydrogen absorption at 200 °C of ball-milled mixtures (Mg + Ni and Mg + Pd) and SCF samples (Mg + Ni and Mg + Pd) after the 100th hydriding/dehydriding cycle with a 1 min shake every 10 cycles.

good desorption properties as it takes only 15 min to get a full desorption for the nanocrystalline Mg [16]. Almost the same properties have been found for the Mg + Co mixtures but at 20 °C higher in temperature. The best desorption properties were obverved by Liang *et al*. [14] for mixtures containing vanadium. In this case, the full desorption at 300 °C was reached after only 8 min. A mechanism of the catalysis has been proposed and will be described in the next section.

Recently, we succeeded in the deposition of nanoplots of metal on the surface of Mg powder using a supercritical fluid process (SCF). The SEM analysis shown in Fig. 4 confirms the presence of nanoplots. In this case, the catalytic activity of the metal is expected to be higher as the specific surface is larger.

In Fig. 5, the 2nd absorption cycles of Mg + Ni and Mg + Pd mixtures ball-milled and decorated by supercritical fluid (SCF) at 200 °C is presented. Both Pd and Ni improve the absorption kinetics, but Ni has a larger effect. The Pd catalytic effect has been examined by other authors [16 – 20]. The Pd is often used in the form of thin films [17], but recently it has been de-

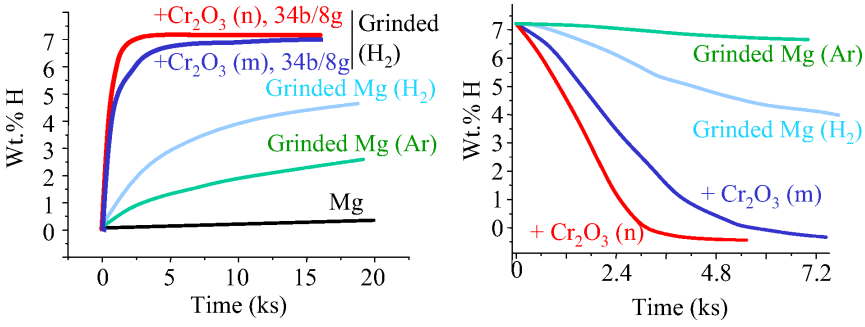


Fig. 6. Absorption kinetics (left) at 473 K (200 °C) and 1 MPa and desorption kinetics (right) at 553 K (280 °C) at 0.03 MPa for unmilled Mg, Mg milled under Ar and $H_2$, and milled under $H_2$ with 5 % $Cr_2O_3$ (nano or micro) additives.

posited on the surface of magnesium using the polyol process [18]. The desorption was complete after approximately 30 minutes at 300 °C. Finally, Gutfleisch *et al.* [19] prepared a mixture of Mg + 1 % Ni + 0.2 % Pd and could (i) fully absorb hydrogen in less than 10 min at 300 °C, and (ii) absorb 5 wt. % of hydrogen at 200 °C within 60 min. The latter results coincide with ours in the case of Mg + Ni (SCF) where complete absorption is reached after 12 min at 300 °C and after 65 min at 200 °C, while the full desorption is reached after 7 min at 330 °C and after 28 min at 300 °C. However, the results obtained by Janot *et al.* are much better than our results and the difference is not explainable at the present time. Many results exist for Mg + Ni mixtures [16, 20 – 21] and the best values published fit well with those obtained by ourselves. In this study we observed absorption at temperatures as low as 100 °C, and the minimum desorption temperature was 260 °C (under 0.02 MPa). It is also surprising that the ball-milled sample and the SCF sample exhibit almost the same behaviour. As the particle size of Mg is much smaller for samples prepared by ball milling, this materials can be expected to have enhanced kinetics. However, the particle size of Mg prepared by SCF must also be reduced and therefore the size effect may not be predominant in this case.

The cyclability was also investigated. For this purpose, and to replicate conditions of use in a tank as best as possible (for mobile application), the samples were shaken with a modified Spex 8000 vibratory miller for 1 min every 10 hydriding/dehydriding cycles. The absorption behaviour of the samples after 100 cycles (after 10 shakes) is reported in Fig. 5. The difference between the absorption after the 2$^{nd}$ and the 100$^{th}$ cycle is mainly the smaller decrease of the kinetics for the SCF samples as compared with the ball-milled sample. Moreover, we also noticed a difference in the activation energy of nucleation after 100 cycles, meaning that the catalytic effect of metals decreases for ball-milled samples whereas it remains almost constant for SCF samples. The large decrease of the diffusion coefficient after the 100$^{th}$ cycle is probably due to crystal growth occurring as the cycle was carried out at 250 °C for absorption and at 300 °C for desorption. The sintering of the materials leads to larger particles and thus to lower diffusion coefficients. However, as for the 2$^{nd}$ cycle, no difference between the diffusion coefficient of both SCF and ball-milled samples can be observed. This indicated that the cycling did not have any effects on the diffusion process (except the sintering effect already mentioned). The good cyclability of SCF samples is explained by the formation of chemical bonding between Mg and the catalyst (deposited by SCF). Such chemical bonding apparently is stronger in SCF samples than in the samples obtained by mechanical grinding (MG).

Starting six years ago, interest has also been focused on the addition of oxides. The first work by Oelerich *et al.* [8] showed a great improvement of the kinetics in both absorption and desorption processes. Our own interest focused on the addition of $Cr_2O_3$ and especially on the effects of nanosized $Cr_2O_3$. The respective absorption and desorption kinetics are shown in Fig. 6.

According to the Ellingham diagram, $Cr_2O_3$ should be reduced by Mg with concomitant formation of MgO. Such reduction has been reported after a hydriding/dehydriding cycle of a Mg + $Cr_2O_3$ mixture [22], but Oelerich *et al.* [8] as well as ourselves did not observe any reduction during the milling process. The kinetics of the reduction is dependent on the temperature and is probably very low at r. t. (*i. e.* the milling temperature). Recently, Dehouche *et al.* [23] reported that the change of hydriding/dehydriding properties during cycling was due to the reduction of $Cr_2O_3$ to Cr metal. The zeta potential measurements (mainly due to the $Cr^{3+}$ ion present in the Mg-based mixture) performed

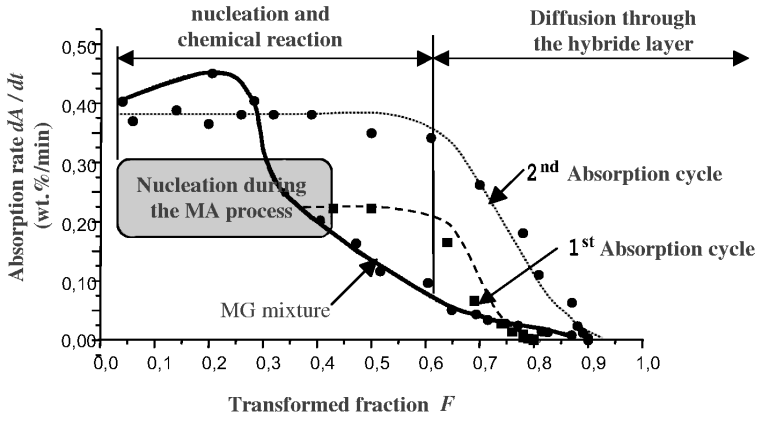


Fig. 7. Absorption rate for the products submitted to RMG (dotted lines) and MA (MG).

Table 1. Desorption rates at 300 °C for different mixtures.

| Mixtures | Milling conditions | Desorption rate (wt. % $s^{-1}$) | Reference |
|---|---|---|---|
| Mg | 200 rpm, 17 balls, 8 h | $0.05 \times 10^{-2}$ | this work |
| Mg + 5 % $Cr_2O_3$ | 200 rpm, 17 balls, 8 h | $0.69 \times 10^{-2}$ | this work |
| Mg + 5 % $Cr_2O_3$ | 300 rpm, 17 balls, 8 h | $0.89 \times 10^{-2}$ | this work |
| Mg + 5 % $Cr_2O_3$ | 300 rpm, 34 balls,10 h | $1.32 \times 10^{-2}$ | this work |
| Mg + $Cr_2O_3$ nano | 300 rpm, 34 balls,10 h | $2.54 \times 10^{-2}$ | this work |
| Mg + $Cr_2O_3$ | 300 rpm, 120 h | $1.52 \times 10^{-2}$ | [8] |
| Mg + $Nb_2O_5$ | 300 rpm, 120 h | $10.2 \times 10^{-2}$ | [24, 25] |

on both Mg + $Cr_2O_3$ and $Cr_2O_3$ SCF-ground for different milling times indicates that some $Cr^{3+}$ could be reduced to Cr metal in the case of the Mg + $Cr_2O_3$ SCF mixture as the zeta potential is decreasing. The presence of Cr atoms or clusters could play an important role in the absorption properties, though.

The absorption properties reported here are very close to those obtained by Oelerich *et al.* [8] for nanocomposite $MgH_2$ / $Cr_2O_3$ mixtures. Significant absorption is obtained at temperatures as low as 200 °C (*i. e.* almost 3 wt. % after only 1 minute).

The use of SCF-ground $Cr_2O_3$ as compared to that of $Cr_2O_3$ leads to an improvement of the desorption kinetics. In the third desorption cycle, more than 50 % of the hydrogen (approximately 3.5 wt. %) is desorbed after 30 min, whereas it takes more than 45 min for the mixture with $Cr_2O_3$. However, the desorption kinetics were not as good as those obtained for nanocomposite $MgH_2$ / $Nb_2O_5$ mixtures [8]. Nevertheless, a comparison of the first two lines of Table 1 shows that the effect of $Cr_2O_3$ addition is huge (compared with the effect of ball milling). Simply by optimizing the milling conditions (from line 2 to line 4) it is possible to almost double the desorption rate. Using nano $Cr_2O_3$ leads to an increase of the desorption rate (*e. g.* $2.54 \times 10^{-2}$ wt. % $s^{-1}$). In this case the kinetics obtained are even higher than the best ones published previously for the same system [8, 24 – 25]. This clearly highlights that the optimization of the production of $MgH_2$ composite powders is still in progress and the industrialization should take that into account (for preindustrialization, see ref. [26]).

*Absorption kinetic analysis*

Several hypotheses on the mechanism of the absorption phenomenon have already been proposed. A good review on the different laws which can be applied can be found in [27 – 28]. In this paper, we take as an example the Mg + Co mixtures and establish the influence of 'reactive mechanical grinding' (RMG). The plot $dA/dt = f(F)$ presented in Fig. 7, where $A$ is the weight % of hydrogen absorbed (which is equivalent to a graph $dF/dt = f(F)$ where $F$ is the fraction of $MgH_2$ formed) and $t$ is the time of hydrogenation, allows a better understanding of the influence of the MA atmosphere (the terms MA for 'mechanical alloying' or MG for 'mechanical grinding' are used synonymously). The rate of formation is initially steady indicating that the reaction is controlled by a nucleation process, followed by a rapidly decreasing reaction rate, indicating that the reaction is controlled by a diffusion process. The nucleation process exists even for the first cycle but starts at around $F = 0.4$ because of the *in situ* hydrogenation that occurred during the RMG. The behaviour reported for MA products is equivalent, but in this case the nucleation duration (length) is shorter. Moreover, during the first absorption cycle, the reaction rate is very slow and typical of a reaction controlled by nucleation and growth. The two-step behaviour is only observed from the second

cycle on. It is also noticed that the length of the nucleation process is increasing slightly with the number of hydrogenation cycles. A direct relationship between the specific surface and the nucleation duration can be established. Such a direct relationship clearly proves that the process involved in the first step of the hydrogenation is controlled by the surface (as the nucleation process is). As the number of hydrogenation cycles increases, the specific surface likewise increases (a decrepitation phenomenon) which leads to a longer nucleation duration. With a longer milling time the specific surface increases and thereby the nucleation duration. However, beyond 10 h, the specific surface is not increased any further. To characterize the second step process, we use a simple model (spherical moving boundary model [29]). The rate equation can be written as:

$$\frac{\mathrm{d}F}{\mathrm{d}t} = \frac{4\pi r k D_{\mathrm{H}}({P_0}^{1/2} - {P_{\mathrm{eq}}}^{1/2})}{((1-F)^{-1/3} - 1)}$$
$$\text{and} \quad C = k D_{\mathrm{H}}({P_0}^{1/2} - {P_{\mathrm{eq}}}^{1/2})$$

where $r$ is the crystallite radius, $k$ the rate constant which depends on temperature and pressure, $P_{\mathrm{o}}$ the applied pressure and $P_{\mathrm{eq}}$ the equilibrium pressure (calculated according to the thermodynamic properties published by Liang *et al.* [12] (*i. e.* $\ln P_{\mathrm{eq}} = -\frac{74400}{RT} + \frac{133.5}{r}$).

In order to compare all of the mixtures, we took the Mg RMG-treated for 2 h as a reference product and normalized the $C$ value estimated for the Mg + 10 wt. % Co mixture by the $C$ value calculated for this reference. Then, as the milling conditions are the same for all experiments and as, at given temperature and pressure, $k$ and $({P_{\mathrm{o}}}^{1/2} - {P_{\mathrm{eq}}}^{1/2})$ should be constant (even if some dependence on the milling time exists), the normalized $C$ values give us the opportunity to compare the diffusion process.

It is observed that the diffusion is improved by increasing the milling time up to 10 h as expected from the creation of defects. Beyond 10 h, the milling has been reported to be almost ineffective (no more internal stress generated), and hence no more improvement of the diffusion constant is observed. The addition of Co does not improve the diffusion process which means that the *3d* element acts as a catalyst for the dissociation of $H_2$ as reported in other studies [13, 20, 22]. The use of RMG (compared with MA) leads to the largest improvement of the diffusion process. In the case of RMG we established a linear relationship between the number of crystallites per particle and the normalized coefficient. This relationship does not exist for the MA products suggesting two different behaviours. To a first approximation, we could conclude that the driving force of diffusion in the case of the MA product is the *intra*-grain diffusion as shown by Zaluska *et al.* [30], and that in the case of the RMG product the *inter*-grain diffusion should not be considered as negligible.

### *The current development of the $MgH_2$ tank*

Over the past years there has been a number of attempts to establish the use of $MgH_2$ in a hydrogen tank. Few laboratories have been working in that direction and some companies (especially two: Hera, a branch of Hydro Quebec, and MCP Technology, a French company) have also been involved in the development of such tanks. In collaboration with the Laboratoire de Cristallographie (and especially the team of Dr. Fruchart), MCP Technology has developed a hydrogen tank [26] that can be filled with few kilograms of $MgH_2$. In performing the scale up of ball milling from the laboratory scale to the industry scale, it has been shown that the milling energy achieved in the larger miller is so high that the milling time could be reduced drastically. The performance of the $MgH_2$ in the tank was excellent, and it has been shown that the absorption can take place at rather low temperatures (*i. e.* 200 to 250 °C). However, the desorption requires substantially higher temperatures (*i. e.* 350 to 400 °C). The most serious problem regarding the use of such a tank was the thermal one. The absorption process is highly exothermic so that during the absorption process, the temperature increase is very high (about 20 to 30 °C) but not uniform in the tank. Correspondingly, the desorption process is endothermic so that large energies are required in order to compensate the decrease in temperature during the desorption process. It has even been reported that the decrease of temperature can be so high that the desorption process stops. It is thus clear that the major improvement needed is not so much on the $MgH_2$ powder properties but mainly on the heat exchange properties during both absorption and desorption processes. In refs. [26, 31 – 32] some thermal drains have been evaluated. For example in ref. [26], a copper tube (with a cooling fluid flowing in it) was introduced in the tank. In the case of water-

cooled systems, the cooling was so efficient that the absorption stopped when only 3.65 wt. % of hydrogen had been absorbed. A pressurized air flow is efficient enough to remove the heat generated by the absorption without stopping the process. An absorption of 4.9 wt. % in less than 30 min at 280 °C was observed. In this last case, the tank could even be plugged to a fuel cell to produce the electricity needed for a helmet front light. Even if such a system will probably never be in use, it proves the possibility of using $MgH_2$ tanks to connect to a fuel cell.

## Conclusions

In the first section, the improvement of the hydrogen absorption kinetics of Mg and $MgH_2$ powders has been reviewed. Milling processes allow the production of nanocrystalline powders with improved properties. The addition of metal (*e. g*. Ni or Co) or oxides ($Cr_2O_3$ or $Nb_2O_5$) also leads to a great improvement in the kinetics. In the case of Ni it is concluded that the catalytic effect on the dissociation of $H_2$ is responsible for the improvement. For the oxides, the highest increase in the kinetics is obtained with oxides containing a metal with different valence states. However, this assumption has not been confirmed.

To enhance the catalytic effects, it is necessary to increase the specific surface of the catalyst. For that purpose, nano $Cr_2O_3$ has been used and, as expected, leads to further improved kinetics superior to the addition of macro $Cr_2O_3$. Such behaviour opens a new research field, and nano metal deposition on the Mg powder is currently under development.

The development of tanks filled with $MgH_2$ powder has become a reality and it appears that the main problem is the heat exchange during absorption (heat dissipation) and desorption (heating) process. Thermal drains, such as expanded natural graphite or metallic foam, are presently under testing and are expected to improve the behaviour of the $MgH_2$ tanks. The current development of thermal drains for electronic devices could also be of great help.


[1] H. Nagai, H. Tomizawa, T. Ogasawara, W. Shoji, *J. Less-Common Met*. **1990**, *157*, 15 – 24.

[2] N. Gerard, S. Ono, in: *Hydrogen in Intermetallic Compounds II* (Ed. L. Schlapbach), Springer, Berlin, **1992**, p. 178.

[3] E. Gaffet, O. Tillement, *Ann. Chim. Sci. Mat*. **1997**, *22*, 417 – 422.

[4] I. G. Konstanchuk, E. Y. Ivanov, M. Pezat, B. Darriet, V. V. Boldyrev, P. Hagenmuller, *J. Less-Common Met*. **1987**, *131*, 181 – 189.

[5] S. Orimo, K. Ikeda, H. Fuji, K. Yamamoto, *J. Alloys Compd*. **1997**, *260*, 143 – 146.

[6] M. Terzieva, M. Khrussanova, P. Pechev, D. Radev, *Int. J. Hydr. Energy* **1995**, *20*, 53 – 58.

[7] G. Alefed, J. Völkl, *Hydrogen in Metals*, Springer, Berlin, **1978**.

[8] W. Oelerich, T. Klassen, R. Bormann, *J. Alloys Compd*. **2001**, *315*, 237 – 241.

[9] J.-L. Bobet, S. Desmoulins-Krawiec, E. Grigorova, F. Cansell, B. Chevalier, *J. Alloys Compd*. **2003**, *351*, 217 – 221.

[10] G. Barkhordarian, T. Klassen, R. Bormann, *Scripta Mater*. **2003**, *49*, 213 – 217.

[11] J.-L. Bobet, S. Pechev, B. Chevalier, B. Darriet, *J. Mater. Chem*. **1999**, *9*, 315 – 318.

[12] G. Liang, J. Huot, S. Boily, A. Van Neste, R. Schulz, *J. Alloys Compd*. **1999**, *291*, 295 – 299.

[13] A. Zaluska, L. Zaluski, J. O. Ström-Olsen, *J. Alloys Compd*. **1999**, *288*, 217 – 225.

[14] G. Liang, J. Huot, S. Boily, R. Schulz, *J. Alloys Compd*. **2000**, *305*, 239 – 245.

[15] J. Rodriguez-Carvajal, FULLPROF, A Program for Rietveld Refinement and Pattern Matching Analysis, Satellite Meeting on Powder Diffraction of the 15th International Congress of the IUCr, Toulouse (France) **1990**.

[16] R. Vijay, R. Sundaresan, M. P. Maiya, S. Srinivasa Murthy, *Int. J. Hydr. Energy* **2005**, *30*, 501 – 508.

[17] R. A. H. Niessen, P. Vermeulen, P. H. L. Notten, *Electrochim. Acta* **2006**, *51*, 2427 – 2436.

[18] R. Janot, X. Darok, A. Rougier, L. Aymard, G. A. Nazri, J.-M. Tarascon, *J. Alloys Compd*. **2005**, *404 – 406*, 293 – 296.

[19] O. Gutfleisch, S. Dal Toè, M. Herrich, A. Handstein, A. Pratt, *J. Alloys Compd*. **2005**, *404 – 406*, 413 – 416.

[20] J.-L. Bobet, E. Akiba, Y. Nakamura, B. Darriet, *Int. J. Hydr. Energy* **2000**, *25*, 987 – 996.

[21] N. Cui, P. He, J. L. Luo, *Acta Mater*. **1999**, *47*, 3737 – 3743.

[22] M. Y. Song, J.-L. Bobet, B. Darriet, *J. Alloys Compd*. **2002**, *340*, 256 – 262.

[23] Z. Dehouche, T. Klassen, W. Oelerich, J. Goyette, T. K. Bose, R. Schulz, World Hydrogen Energy Congress, Montreal (Canada) **2002**.

[24] O. Friedrichs, F. Aguey-Zinsou, J. R. Ares Fernandez, J. C. Sanchez-Lopez, A. Justo, T. Klassen, R. Bormann, A. Fernandez, *Acta Mater*. **2006**, *54*, 105 – 110.

[25] G. Barkhordarian, T. Klassen, R. Bormann, *Scripta. Mater*. **2003**, *49*, 213 – 217.
[26] P. de Rango, A. Chaise, J. Charbonnier, D. Fruchart, M. Jehan, P. Marty, S. Miraglia, S. Rivoirard, N. Skryabina, *J. Alloys Compd*. **2007**, doi:10.1016/j.jallcom.2007.01.108.
[27] G. Barkhordarian, T. Klassen, R. Bormann, *J. Alloys Compd*. **2004**, *364*, 242 – 246
[28] J.-L. Bobet, M. Kandavel, S. Ramaprabhu, *J. Mater. Res*. **2006**, *21*, 1747 – 1752.
[29] M. Y. Song, J. Y. Lee, *Int. J. Hydr. Energy* **1983**, *8*, 363 – 367.
[30] A. Zaluska, L. Zaluski, J. O. Ström-Olsen, *Appl. Phys. A* **2001**, *72*, 157 – 165.
[31] P. Benard, V. Mustafa, D. R. Hay, *Int. J. Hydr. Energy* **1999**, *24*, 489 – 495.
[32] P. Marty, J.-F. Fourmigue, P. de Rango, D. Fruchart, J. Charbonnier, *Energy Conversion and Management* **2006**, *47*, 3632 – 3643.